Homing of canine multipotent mesenchymal stromal cells after epidural transplant in acute spinal cord injury in rabbits

Mariana C. Ramos,[1] Diego N. R. Sánchez[1], Giovanna B. A. Pinto[1], Felipe J. Sanches[1] , Matheus Bertanha[2], Lenize d. S. Rodrigues[2], Alexandre L.R. de Oliveira[3], André L. Bombeiro[3], Emerson G. M. de Siqueira[4], Carlos E. F. Alves[5], Alexandre Battazza[5], Rogério M. Amorim,[1]

[1] Veterinary clinic, UNESP, Botucatu, 18618-687, Brazil.
[2] surgery and orthopedia, UNESP, Botucatu, 18618-687, Brazil.

[3] Department, UNICAMP, Campinas, 13083-862, Brazil.
[4] Veterinary surgery, UNESP, Botucatu, 18618-687, Brazil.

[5] Veterinary Pathology, UNESP, Botucatu, 18618-687, Brazil.

Correspondence should be addressed to Rogério M. Amorim;
rogerio.amorim@unesp.br.

Abstract

Multipotent mesenchymal stromal cells (MSC) have been presented by the scientific community as a promising alternative in the treatment of inflammatory, traumatic, vascular and degenerative diseases of the central nervous system due to their anti-inflammatory, immunomodulatory and neuroregenerative properties. One of the aspects that can affect the effectiveness of the stem cell therapy is the transplantation route used. The aim of this study was to evaluate the homing of canine adipose derived MSCs (AdMSCs) transplanted via epidural injection in an experimental model of acute spinal cord injury in rabbits. New Zealand rabbits (n=8) were subjected to the spinal cord injury induced by compression of the 10^{th} thoracic segment. Immediatily after the surgical procedure, the animals were submitted to the transplantation of marked AdMSCs with quantum dots through epidural injection between the L7-S1 spaces. Seven days after the transplant, the brain, spinal cord, lungs, kidney, spleen and liver were collected and evaluated by bioluminescence imaging. The spinal cord segments L7-S1 and thoracic injury site were evaluated by confocal microscopy to identify the presence of marked canine AdMSCs. Results shows that AdMSCs migrate to thoracic spinal cord segment, lungs, brain, liver and kidneys, no bioluminescence was observed in spleen. The presence of canine AdMSCs in spinal cord indicates the capacity of these cells to overcome the dura mater and reach the transplantation site. The epidural delivery is feasible and minimally invasive and might be a good candidate for cell transplantation in the context of neurological diseases.

Keywords: stem cell tracking, xenotransplant, epidural transplantation, spinal cord injury, mesenchymal stromal cells.

INTRODUCTION

Multipotent mesenchymal stromal cells (also known as mesenchymal stem cells - MSCs) are promising approach for the treatment of inflammatory, degenerative, neurological and cardiovascular diseases due to their immunomodulatory and regenerative potential.

The use of MSCs has been widely studied in spinal cord injury models and in preclinical trials with good results reported in terms of morphological and functional improvement after traumatic, ischemic and inflammatory injuries [1,2,3,4,5,6,7].

Homing is the process by which MSCs reach the target site anfter transmigration across the endothelium [8]. This process has been considered crucial for the effectiveness of stem cell therapy, since the mechanism of action of MSCs is presumably linked to their ability to produce factors that act in paracrine or justacrine manner to the target cell. Thus, the closer the MSCs are to the injured tissue, better results are expected [9,10,11,12].

Little is known about the exact mechanisms that MSC utilize to reach the target tissue, however many growth factors and cytokines have already been identified as being active in the process, such as VEGF-A, HGF, TGF-β1, TNF-α, SDF- 1 α, IL-6, IL-8, IGF 1, and receptors, adhesion molecules and metaloproteinases such as CXCL-12, CCL-2, CCL-3, CCR4, CXC44, VCAM, ICAM [13,14,15,16].

The data are still scarce and controversial about the fate of MSCs after carrying out cell transplantation through different routes. When the intravenous route is used, a large concentration of these cells is observed in the lung [17,18,19] following the systemic distribution of part of these cells and their subsequent disappearance.

In order to circumvent the trapping of cells in pulmonary capillaries and encourage more cells to migrate to the injured spinal cord, many authors have used transplants close to the injury site, through the intralesional, intrathecal or interventricular injections [20,21].

However, direct transplantation to the injured spinal cord leads to an additional risk to the procedure, distributes the cells in a hostile environment

and is potentially clinically unfeasible because it is necessary to subject the patient to an anesthetic and surgical procedure [22].

Therefore, transplantation pathways that ensure that cells are delivered close to the lesion site and that favor them crossing the blood-brain barrier are essential [14, 23, 3].

The epidural injection is an alternative for MSCs transplantation for neurological diseases because it is less invasive and has already been extensively studied related with drugs delivery in anesthesia and chronic pain control, providing good distribution of the drugs used [24].

Still on drugs administered by this route, their systemic absorption occurs through diffusion through epidural fat and ligaments. Locally it spreads through the spinal meninges reaching the subarachnoid space, up to the cerebrospinal fluid (CSF), where it is distributed throughout the spinal cord and brain using the cerebrospinal fluid flow. The greatest barrier to the local diffusion of these drugs is the arachnoid mater [25,26].

In this context the aim of this study was evaluate canine Adipose derived MSCs (AdMSC) homing after epidural transplantation in a model of acute spinal cord injury in rabbits. It is necessary to evaluate the applicability and effectiveness of transplanted cells and to promote the homing of MSCs to a neurological system injury site before this technique is widely used in clinical contexts of neurological diseases, such as spinal cord injuries.

We hypothesized that canine AdMSCs transplanted by epidural route are able to distribute themselves systemically and locally and reach the spinal cord injury site.

MATERIALS AND METHODS

Experimental design

This study was approved by the Ethics Committee on Animal Experimentation, previously established by COBEA (Brazilian College of Animal Experimentation), as stated in the protocol CEUA-FMB-Unesp, nº 1286/2019.

Eight male and female rabbits from the Botucatu Genetic Group were used, from the Central Animal Farm of UNESP - Campus Botucatu, weighing between 2.5 - 4.0 kg and approximately 6 months of age.

The animals were kept in individual cages with dimensions of 55 x 55 x 55 cm and suspended 80 cm from the floor. The room temperature was maintained at 20ºC and with 12-hour light cycles, they received comercial diet (Nutricoelhos, Purina Nutrimentos Ltda.), water ad libitum during the entire study period. During the three-day postoperative period the animals also received green leaves (kale) and were kept under the care of specialized technicians.

Canine AdMSC immunophenotyping and multipotentiality assays

The cells were obtained from the adipose tissue of healthy dogs from elective surgeries. The adipose tissue samples were stored in Hank's Balanced salt solution (HBSS) (Invitrogen, Carlsbad, CA, USA) and divided into fragments (1-2 mm^3) to be digested with collagenase type 1A (Sigma Aldrich, St Louis, MO, USA). They were kept at 37 ºC and stirred every 10 minutes for 1-2 hours.

After neutralizing the enzyme with 10% fetal bovine serum (SFB) (Sigma-Aldrich, Saint Louis, MO, USA), the material was filtered and centrifuged to separate the cell pellet. The cells obtained were divided into 25 cm^2 bottles with 6 ml of medium, incubated at 37ºC in a humid atmosphere, containing 95% air and 5% CO_2.

The culture medium was prepared with Dulbecco's Modified Eagle, Medium Nutrient Mixture F-12 (DMEM/F-12 Gibco; Thermo Fisher Scientific, Grand Island, NY, USA), 10% SFB, 1% penicillin / streptomycin, 1.2 % amphotericin (Sigma-Aldrich, St. Louis, MO, USA), and changed after the first 48 hours and then every 3 to 4 days.

The cells were trypsinized (trypsin, 0.25%, Gibco; Thermo Fisher Scientific) when they reached 80% confluence. As soon as the cell population

was isolated, in the third passage the MSCs were characterized by multipotentiality tests and immunophenotypic labeling. The cells samples used were previosly characterized.

Canine cells were evaluated for surface markers in reactions containing species-specific antibodies for rats that included: CD 90-PERCP (BD, Pharmigen ™, San Diego, CA, USA), CD 71-FITC (BD Pharmigen ™, San Diego, CA, USA), CD 45-PE (BD Pharmigen ™, San Diego, CA, USA), CD 106-PE (Abcam, Cambridge, MA, USA), CD11b-APC (Abcam, Cambridge , MA, USA), and CD 34-FITC (Biorbyt ™, St Louis, MO, USA). Canine MSCs were analyzed on the BD FACSCalibur flow cytometer (Becton Dickinson Company, San Jose, USA).

Cell suspensions at a concentration of $1x10^6$ cells diluted in 100 µL of saline were used and conjugated antibodies were added to the solution according to manufacturer's recommendations. After the analysis, the data were evaluated by the Cell Quest Pro software (Becton Dickinson Company, San Jose, USA).

In order to confirm multipotentiality, cultured cells were induced to differentiate in vitro into adipogenic, chondrogenic and osteogenic strains, with the StemPro adipogenesis®, chondrogenesis® and ostegenesis® differentiation sets (Gibco; Thermo Fisher Scientific, Grand Island, NY, USA) following the manufacturer's recommendations.

Passage two to six were used in *in vivo* experiments

Canine AdMSC labelling with quantum dots

Prior to cell transplantation, cells were trypsinized and marked with a Qtracker 655® marker (Cell labeling kit, Molecular Probes, OR, USA cat code: Q25029) according to the manufacturer's recommendations. The labeled cells were resuspended in 0.3 ml of HBSS at the time of transplantation.

Spinal cord injury model

As anesthetic protocol, the animals were submitted to pre-anesthetic medication with midazolam (Cristalia, Itapira, SP, Brazil) 2 mg / kg and ketamine (Vetnil, Louveira, SP, Brazil) 30 mg / kg intramuscularly, anesthetic induction with isofluorane in a face mask until tracheal intubation, maintenance with isoflurane (Cristalia, Itapira, SP, Brazil) and inhaled oxygen.

Venous access was obtained by catheterization of the marginal ear vein to maintain fluid therapy with lactated Ringer's solution, analgesic bolus and infusion of analgesic solution containing fentanyl citrate (fentanyl, Janssen-Cilag Farmacêutica, SP, Brazil) (10ug / kg) / h), ketamine (Vetnil, Louveira, SP, Brazil) (0.3 mg / kg / h) and lidocaine (EMS, Hortolândia, SP, Brazil) (3 mg / kg / h).

The animals were kept in prone position for trichotomy and antisepsis of the entire dorsal region, followed by the surgical procedure for dorsal laminectomy between T8 and T9, obtaining a good spinal exposure for the insertion of the Fogarty 3 French catheter (Edwards Lifesciences, CA, USA) and careful advancement through the epidural space to T10, where the balloon was inflated with 1 cm^3 of air for 10 seconds as described by Vanický and colleagues in 2001, enough time to cause a spinal cord injury, then the balloon was deflated and removed from the spinal canal.

The animals received meloxicam (Ouro fino, Cotia, SP, Brazil) subcutaneously 0.5 mg / kg once daily for 3 days, dipyrone (Halex Istar Indústria Farmacêutica Ltda, GO, Brazil) 50 mg / kg every 12 hours for 5 days, gabapentin 30 mg / kg every 12 hours until the end of the procedure, enrofloxacin (União Química, São Paulo, SP, Brazil) was also administered 5 mg / kg once daily for 5 days.

Canine AdMSCs epidural transplantation

The transplant was performed immediately after spinal cord injury and under the same anesthetic protocol described for the surgical procedure. After trichotomy and local antisepsis, the space between L7 and S1 vertebras was puncturated.

The correct needle positioning was verified by the non-observation of CSF in the needle tube, and the aspiration test of the physiological solution drop by negative pressure. the syringe was attached to the needle with the cells in suspension and the application was performed slowly and continuously with 1.5 x 10^6 cells per rabbit suspended in 0.3 ml of HBSS.

Collection and preparation of tissue samples

The rabbits were euthanized with an overdose of thiopental 50 mg/ml (Thiopentax, Cristália, Itapira, SP, Brazil) after seven days of the surgical procedure + transplantation and were immediately perfused intracardiacally with physiological solution followed by 4% paraformaldehyde buffered.

Spinal cord, brain, kidneys, liver, spleen and lungs of each animal were dissected. The organs were stored at 4 °C in 4% paraformaldehyde and washed with 0.2 M PBS to be fully imaged by the FX PRO *in vivo* imager (Bruker, TX, USA).

Cell tracking:

The nanocrystal-labeled MSCs were screened in organs: spinal cord, brain, kidneys, liver, spleen and lungs seven days after the epidural transplant. The *in vivo* imager fluorescence detection method (FX PRO, Bruker, TX, USA) was used. For imaging, the values of 610 excitation wave and 700 emission wave were used with an exposure time of 5 seconds.

The organs were arranged to be imaged side by side, and were analyzed for fluorescence positivity or negativity compared to the same negative control organ, thus avoiding the possibility of autofluorescence. Organs that showed more fluorescence than the negative control were considered positive, those equal to the negative control were considered negative.

Spinal cord (n=8), brain (n=7), liver (n=7), lung (n=7), spleen (n=6), kidney (n=7) were imaged by means of an "*in vivo"* imaging analyser. The same spinal cords were screened for the presence of nanocrystal marked AdMSCs in two different sites, the lesion site and transplantation site (L7-S1 medullary segment).

Morphological analyses:

Confocal microscopy evaluation:

After imaging, the medullary tissue was prepared for analysis using confocal microscopy. The fragments of the segments corresponding to the T10 lesion site and cell transplant site (L7-S1) were stored overnight in 10% and 20% sucrose solutions, sequentially, for cryopreservation. They were frozen in liquid nitrogen and n-hexane to be sectioned longitudinally and transversely by the cryostat, obtaining fragments with 10 µm. The samples were stored in a -80 ºC freezer until use.

After the cleavage of the fragments in 10 µm thick cross sections, the slides were processed and marked with DAPI (4 ′, 6-diamidino-2-phenylindole) (Invitrogen, Carlsbad, CA, USA), and analyzed using confocal microscopy (TCS, SP8, Leica®, Wetzlar, Germany).

For each of the eight animals analyzed by confocal microscopy, two spinal cord cuts were made, one in the L7-S1 portion and the other at the T10 lesion site. Each slide was analyzed in 3 different fields so that at the end it was

possible to make an average of the amount of fluorescence present in the cut in question. The amount of fluorescence in the confocal microscopy images was analyzed using the Image j program.

Hematoxylin and Eosine staining and Immunohistochemistry

Additionally, cuts of the organs were made to perform morphological analyzes by hematoxylin and eosin (HE) staining. The slides were analyzed qualitatively for the presence of hemorrhage and inflammation. Samples were also processed for immunohistochemistry with specific antibody for macrophages.

Immunohistochemical analysis for the assessment of macrophages was carried out according to Franzoni et al. [27], with modifications. Briefly, paraffin blocks of 5 μm were cut, which were stretched in adhesive slides (Starfrost, Knittel). Subsequently, the slides were dewaxed and antigenic recovery was performed with the pH 6.0 citrate solution in the pressure cooker (Pascal, Dako, Carpinteria, CA USA).

The blocking of nonspecific proteins was performed with a ready-to-use commercial solution (Protein Block, Dako, Carpinteria, CA USA) and the blocking of endogenous peroxidase with hydrogen peroxide (Dynamic) at 3%, diluted in methanol (Dynamic). The slides were incubated with the mouse anti-macrophage monoclonal antibody (Clone MAC387, Bio-Rad Laboratories, Hercules, CA, USA) at a 1: 300 dilution, overnight. The secondary antibody conjugated to peroxidase goat anti-mouse (Abcam) was used in the dilution of 1: 300. The reagent 3-3 diaminobenzidine (DAB, Dako, Carpinteria, CA, USA) was used as a chromogen and the samples were stained with Harris hematoxylin.

To analyze the presence of macrophages, five high-magnification fields were evaluated, and the number of positive cells was counted. At the end, the result was presented with a median.

Statistical analysis:

The integrated pixel density variable was assessed in three spinal medullas for normality using statistical tests (Shapiro-Wilk), descriptive statistics and graphic analysis. The t test was performed for unpaired samples. The level of significance assumed was equivalent to * $p < 0.05$, ** $p < 0.01$ and *** $P < 0.001$. The analysis was performed using the software (GraphPad Prism version 8 for Mac, San Diego, California, USA).

RESULTS AND DISCUSSION

Canine cells showed mesenchymal fate and trilineage :

The immunophenotype profile presented by the cells confirms their mesenchymal origin (figure 1). Immunophenotypic analysis demonstrated positive expression for CD 90 (98,13%) and CD 71 (26,44%) and absence of expression for hematopoietic antigens CD45 (2,04%), CD34 (5,90%), CD 106 (8,96%) and CD 11b (0,55%). Surface markers greater than 20% were considered positive.

The induction of *in vitro* differentiation for adipogenic, chondrogenic and osteogenic lines was positive (figure 2). For adipogenic differentiation, deposition of lipid droplets within the cell cytoplasm was observed when stained with Oil Red O stain. For osteogenic differentiation, all samples cultured in the induction medium demonstrated intense extracellular deposition of stained calcium in Alizarin Red S In chondrogenic differentiation, there was formation of micromass stained by Toluidine Blue.

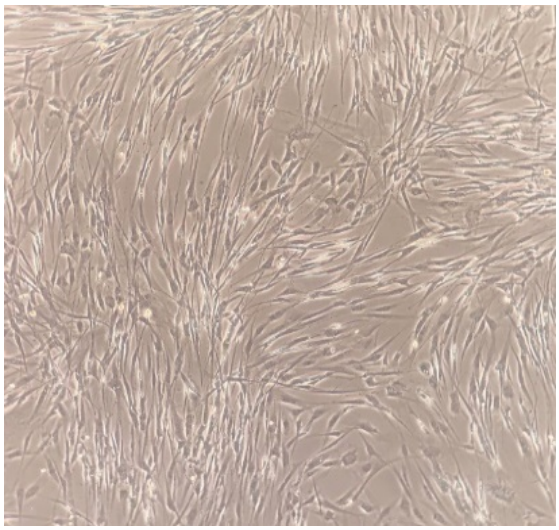

Figure 1. AdMSCs in 20x magnification, 3rd passage. Note fibroblastoid morphology and adherence to plastic.

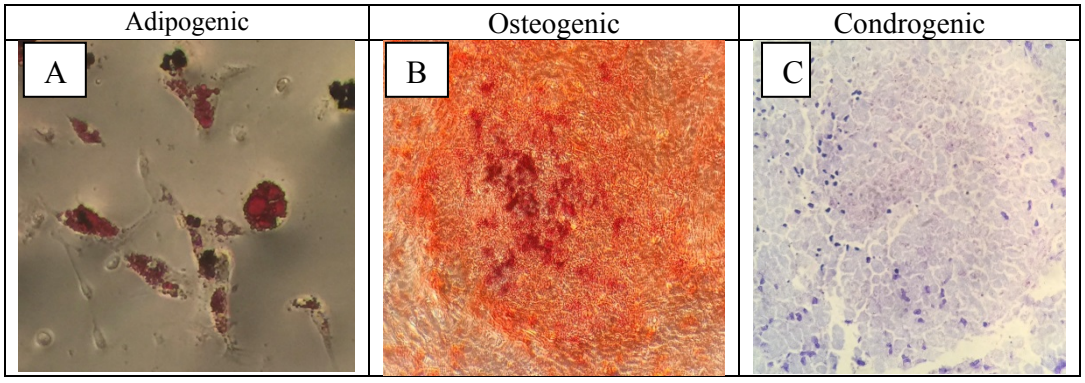

Figure 2. Potential for differentiation of MSC in adipogenic (A), osteogenic (B) and chondrogenic (C) lines, 20x magnification. Note the deposition of lipid droplets within the cell cytoplasm stained with Oil Red O (A). extracellular calcium deposition stained in Alizarin Red S (B). Formation of micromass stained by Toluidine Blue (C).

Histological findinds attests the presence of experimentally induced spinal cord injury

The technique used, adapted from [28] was effective in inducing myelopathy in all animals, characterized by paraparesis, motor deficit and proprioception of the pelvic limbs (Figure 3). The animals showed no deficit in urinary function, but assessing the gait and neurological status or clinical recovery of animals is not the scope of this work, We exclusively analyzed the cellular tracking of AdMSCs.

Figure 3. Rabbit showing motor and proprioceptive deficit of the pelvic limbs after surgically induced spinal cord injury in the thoracic spinal segment

In the morphological evaluation of the spinal cord tissue by hematoxylin and eosin staining, inflammatory changes compatible with the tissue injury caused, such as myelomalacea, congestion and glitter cells were observed (Figure 4). In the brain tissue of some animals, there was the presence of central chromatolysis, perivascular edema and glial nodules, compatible with inflammatory changes. No relevant changes were noted in the spleen, liver, kidneys or lung.

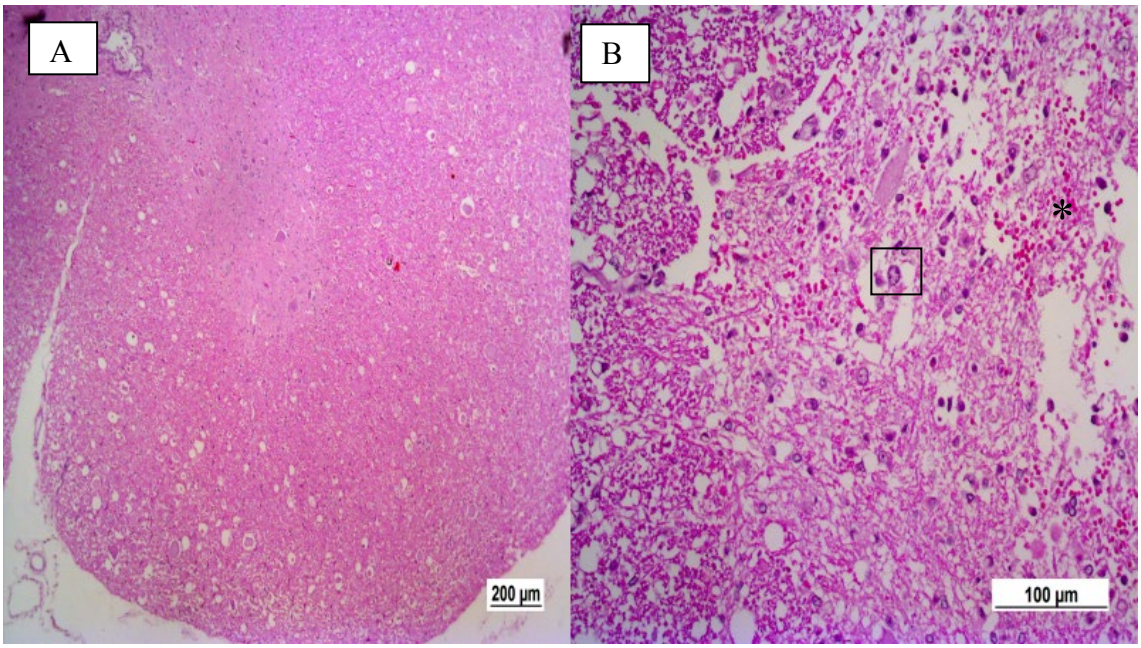

Figure 4. Histological evaluation of the ventral horn of the spinal cord seven days after experimental injury. Figure A: note frequent spheroids and vacuolation of white matter, discrete satellitosis and central chromatolysis, 200 µm scale. Figure B: note frequent spheroid and vacuolization of white matter, central chromatolysis, extensive area of hemorrhagic necrosis (malacia) (asterisk), mainly in gray matter with moderate gitter cells (Square), 100 µm scale.

In immunohistochemical evaluation, samples of liver, lung and kidneys were not positive for macrophages in histological sections. In spinal cords samples, it was possible to identify the presence of macrophages with positive cytoplasmic labeling for the searched antibody. The median staining was 1 macrophage per sample (0 - 15).

Canine AdMSCs migrated sistemicaly and to central nervous system after epidural transplantation

Organs in the imaging analyser were positive for the fluorescent canine AdMSCs in liver (n=6/7), spinal cord (n=2/8), brain (n=6/7), kidney (n=6/7) and lung (n=4/7), and Fluorescence was not observed in any of the imaged spleens (n=6) (figure 6).

Two out of eight spinal cord were positive for canine AdMSCs (Figure 6). Of these two animals, one was positive at the spinal cord injury site and the other one was positive from the proximity of the T10 injury site to the cervical segment (figure 5).

Brains were positive in six of seven imaged animals corresponding to 85.7%, the livers and kidneys were positive in six of the seven animals tested (85.7%). The lungs, on the other hand, showed 57,14% positivity, with four organs positive out of seven imaged (Figure 6).

Despite the low positivity of spinal cords in the imaging analyser, By means of confocal microscopy it was possible to attest to the presence of Qtracker-labeled MSCs in all imaged spinal cords. The confocal was also performed on two brain samples, and it was also possible to confirm the presence of these cells in brain parenchyma as seen at the imaging analyser.

The results of fluorescence imaging of the organs combined with those of confocal microscopy in the present study demonstrate the ability of MSCs derived from canine adipose tissue to distribute systemically from puncture and epidural transplantation between the L7-S1 vertebrae and to reach the nervous tissue.

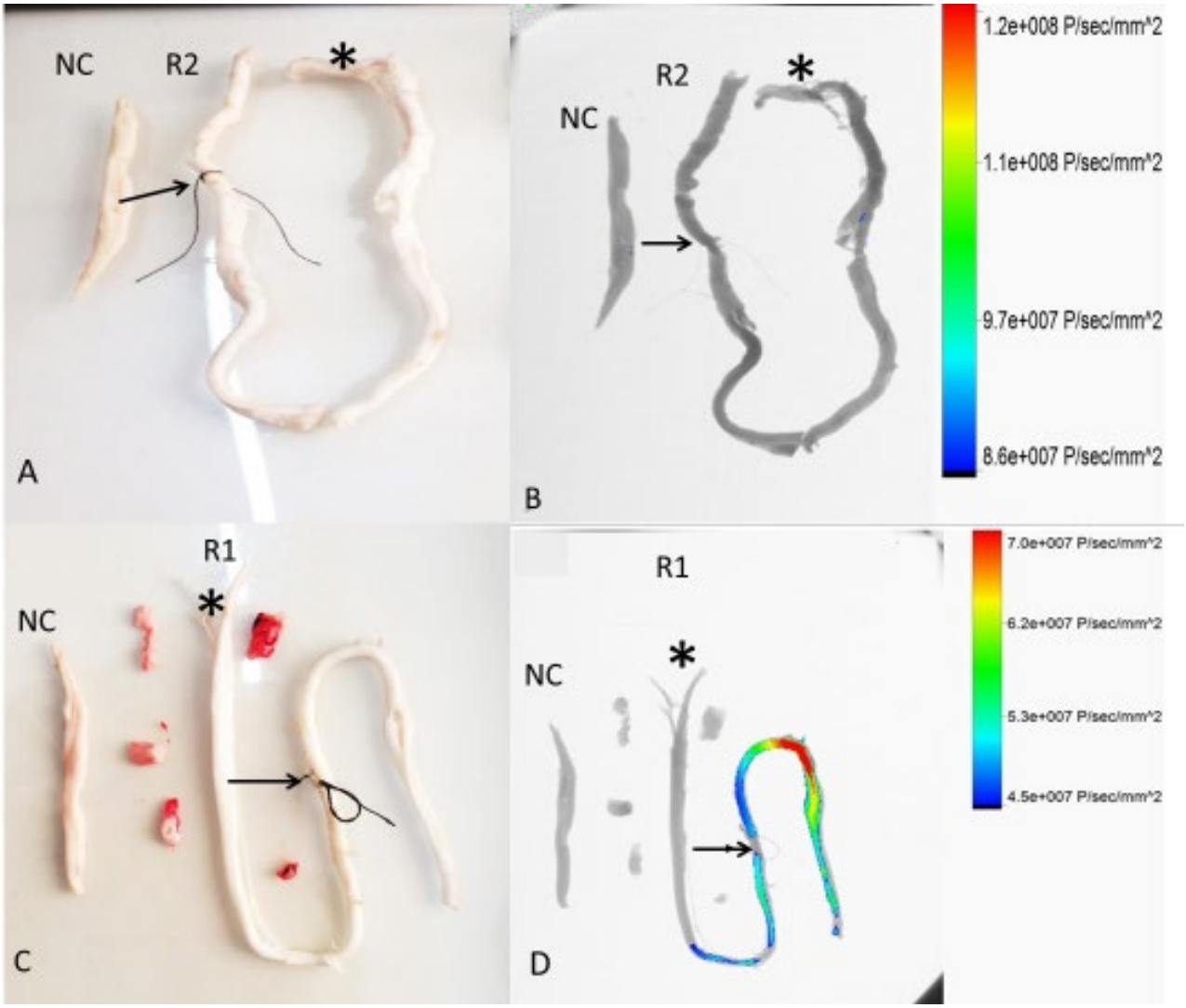

Figure 5. Representation of the spinal cord arrangement in *in vivo* imager. In A and C are pictures of spinal cords of rabbits number one (R1) and two (R2) and their respective negative controls (NC) before being imaged; in B and D the images obtained after the fluorescence analysis of these same rabbits and their respective negative controls are represented. Note that animal number two was negative in the bioluminescence analysis and animal one was positive in the proximal half of the spinal cord. The arrows represent the site of spinal cord injury in T10 and the asterisks the terminal medullary portion, corresponding to L7-S1, a cell transplant site performed by the epidural route.

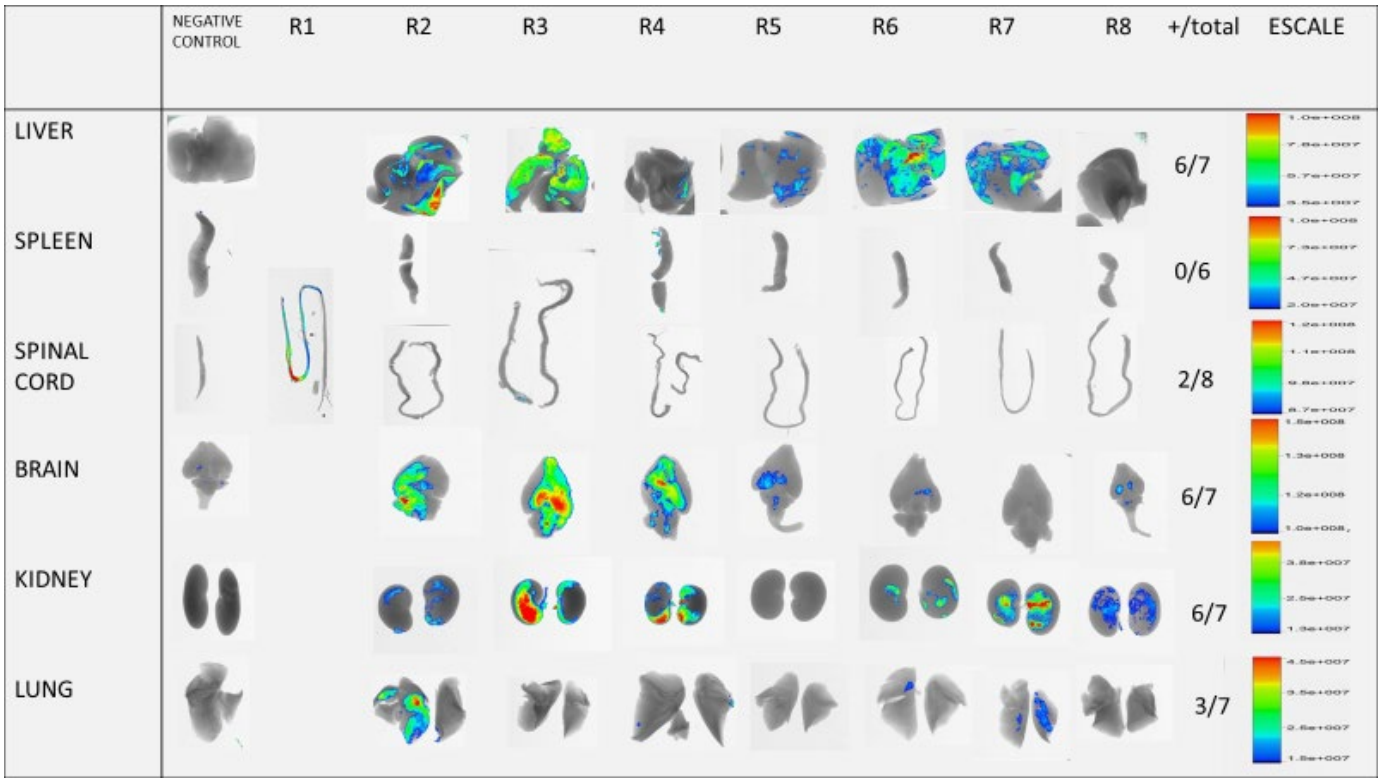

Figure 6. Representation of spinal cords, brain, liver, kidneys, lungs analyzed in *in vivo* imager. On the left, negative control organs, in the middle, organs from rabbits 1 to rabbit 8. Organs that were equal to the negative control were considered negative and those with more fluorescence than their negative control were considered positive. Intensity scale for spinal cord graded from 8.7 x 10^7 to 1.2 x 10^8 photons / second / mm^2, for brain: from 1.0 x 10^8 to 1.5 x 10^8 photons / second / mm^2, for liver from 3.5 x 10^7 to 1.0 x 10^8 photons / second / mm^2, for spleen from 2.0 x10^7 to 1.0 x 10^8 photons / second / mm^2, for lungs from 1, 5 x 10^7 up to 4.5 x 10^7 photons / second / mm^2 and for kidneys from 1.3 x 10^7 up to 5.0 x 10^7 photons / second / mm^2.

Canine AdMSCs migrated sistemicaly and to central nervous system after epidural transplantation, confocal microscopy

As for confocal microscopy, the eight spinal cords were imaged, obtaining images for each animal for the lesion site in the T10 medullary

segment and the site of application of the MSCs in the L7-S1 medullary segment.

Through confocal microscopy, in all of the animals researched by this technique, it was possible to verify the presence of cells marked with nanocrystal in medullary tissue both at the application site in L7-S1 and at the injury site in T10.

Animal number one was not positive in fluorescence imaging for the transplantation site, but MSCs markings in this region were observed by the confocal microscopy technique. Animal number 3 was positive in fluorescence only at the injury site, but through confocal microscopy, marked cells were seen both at the application site and at the injury site (figures 7 and 8). The other spinal cords were negative in bioluminescence chamber but positive for the presence of Qtracker at the injury site and also in the L7-S1 segment in confocal microscopy.

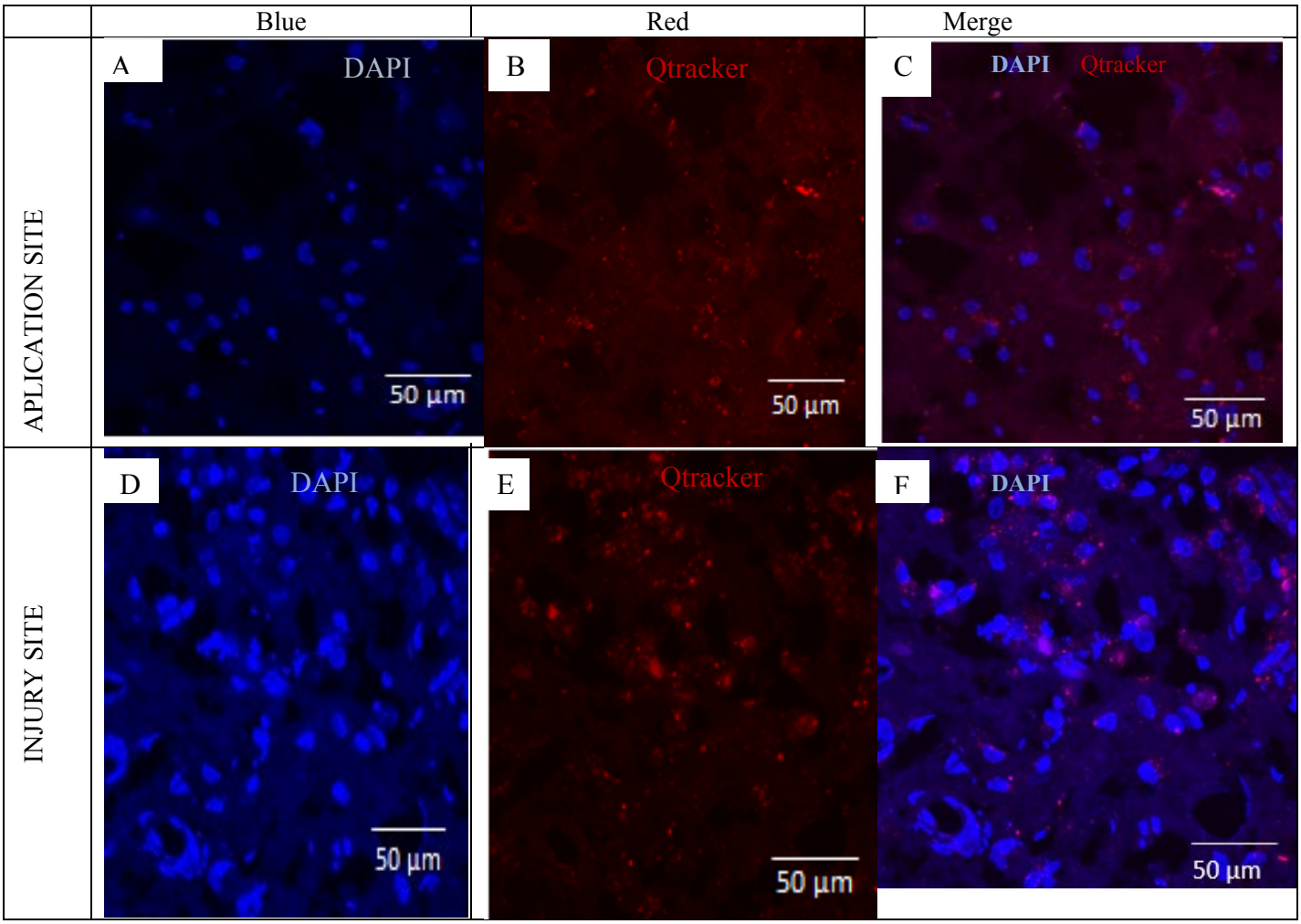

Figure 7. Confocal microscopy images of the spinal cord of animal number 1 in L7-S1 portions (cell transplant site of the MSCs marked with Qtracker 655) and site of spinal cord injury in the T10 segment. In A, section of the application site, note blue fluorescence of the nucleus marking with DAPI staining, in B, note red fluorescence of the Qtracker marker. In C, combined image of the two markings.

In D, section of the spinal cord injury site, note blue fluorescence of the DAPI marker, in E, red marking of the nanocrystal Qtracker 655 and in F image combined with the two markings. Scale 50µm.

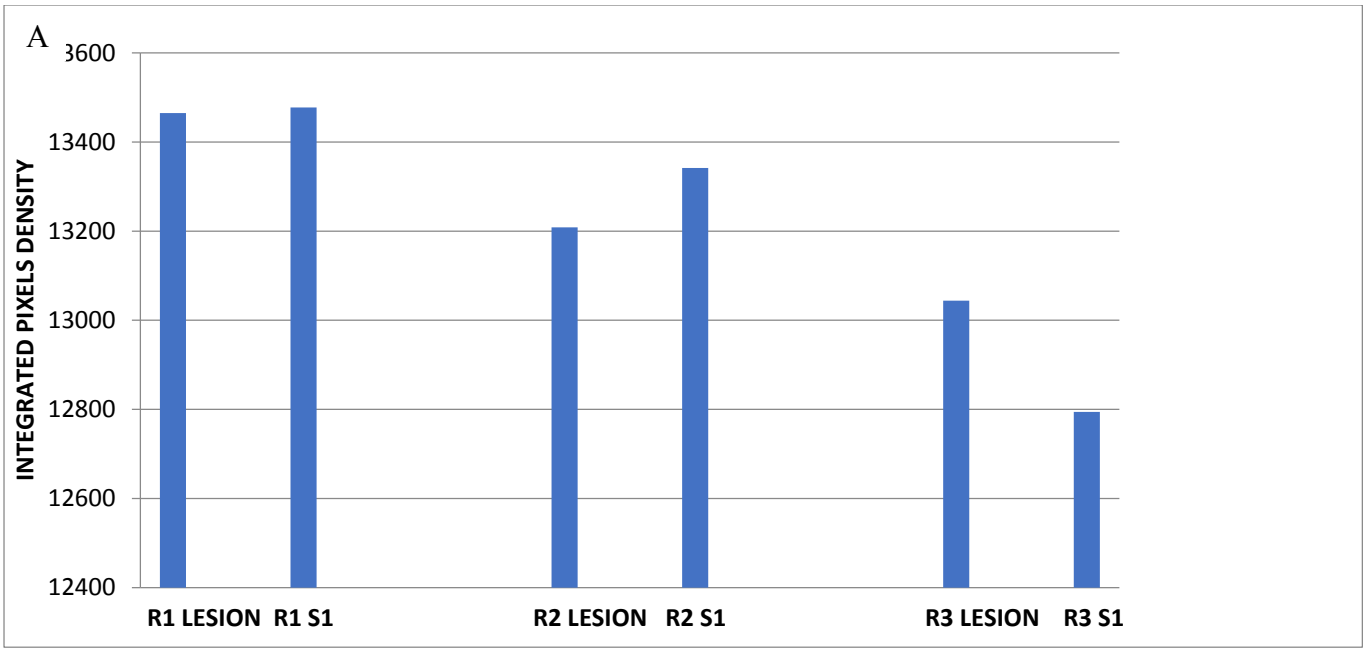

B

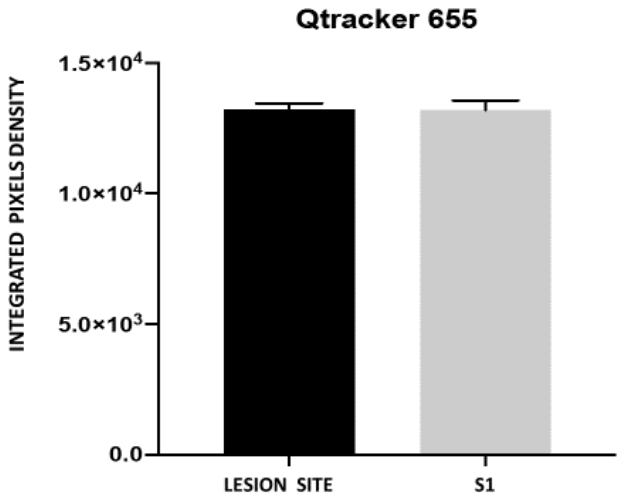

Figure 8. A. Fluorescence intensity of confocal microscopy images of rabbits number 1 (R1), 2 (R2) and 3 (R3) at the injury site and at a cell transplant site in the L7-S1 medullary segment. In B, Quantitative analysis of the fluorescence intensity of canine MSCs marked with Qtracker 655 at the application site and at the spinal cord injury site seven days after the

experimental injury and transplantation. The values of the integrated pixel density were represented as mean ± SD. p> 0.5.

Discussion

Although the mechanisms that govern the cellular homing of MSCs to the injury site are not known for certain, it is known that the presence of tissue damage induces the local production of chemokines that act by attracting MSCs to the injury site through the mechanisms previously explored [8].

We induced a spinal cord injury using the compression model of the arterial embolectomy catheter and evaluated the ability of MSCs to migrate to this spinal cord segment and its distribution to other organs.

Previous studies have demonstrated the ability of MSCs to migrate to the medullary tissue from intrathecal transplantation [20, 21,3]. However, the epidural route by lumbar puncture in the context of transplantation of MSCs is still poorly studied. Bach et al. 2019 [6] published good results for ambulatory improvement of dogs after epidural transplantation of AdMSC, but the transplantation was done at the trans-operative injury site in spinal decompression surgery. To authors' knowledge, the fate of AdMSCs via the epidural route in the L7-S1 intervertebral space has not yet been explored.

The cells marked with nanocrystal transplanted by the epidural route were distributed systemically to kidneys, liver, lung, brain and spinal cord.

The systemic distribution can be explained by the diffusion of cells through epidural fat, vessels and local arteries. The systemic distribution of drugs after epidural injection is well described mainly in the context of the use of anesthetics for surgery or analgesia [25].

Mainly by confocal microscopy, MSCs were observed in the medullary parenchyma, the cells transplanted by epidural route may have been distributed between the meninges up to the CSF, being thus distributed throughout the

medulla. In this process, the arachnoid mater is the main meningeal barrier to diffusion.

In the present study, Qtracker 655 nanocrystals were used as a marker of MSCs due to their ease of internalization in the cell cytoplasm and because of their low cytotoxicity [29]. Good results regarding the traceability of MSCs using the nanocrystal Qtracker have already been reported for bone marrow derived MSCs in a tendonitis model in horses [30].

In vivo imager was used to investigate the presence of nanocrystal labeled MSCs. Imaging by detecting fluorescence *in vivo* has been presented as a good option for tracking of neural stem cells. The technique demonstrated a good relationship between the amount of fluorescence detected and the amount of cells present in the tissue in question.

It could be speculated that the small amount of spinal cord marking by the *in vivo* imager is explained by the use of the transplant through the epidural route and possible difficulty of MSC in crossing the dura mater and reaching the medullary tissue. The amount of fluorescence, and therefore of cells labeled in the spinal cord, needed to be confirmed by confocal microscopy.

Through confocal microscopy, it was possible to verify the presence of cells marked in medullary tissue in all animals, both at the application site and at the injury site. The results of fluorescence imaging of the organs combined with those of confocal microscopy in the present study demonstrate the ability of AdMSC to distribute systemically from puncture and epidural transplantation between the L7-S1 vertebrae and to reach the nervous tissue.

The evidence of fluorescence in kidney, lung, liver and brain organs in the *in vivo* imager device can be explained by the presence of Qtracker-labeled MSC in its cytoplasm in the organ in question. These may have gone through the process of active migration to other target tissues other than the injury site at T10, or they may have gained blood flow through vessels in the epidural region and be sequestered in capillaries and venules, this phenomenon is well described for the lung when the intravenous route is used [19,31].

The time elapsed from the transplant to the tracking for these in the target tissue is important. In our study, we chose to evaluate cell migration seven days after transplantation.

In addition, we also performed an experiment with a rabbit that underwent surgical procedure and cell transplantation with rabbit MSCs via the epidural route as previously described and sacrificed three days after the procedure. The same organs were investigated in this animal and it was verified by the fluorescence imaging the presence of markings only in the lung, corroborating to the possibility of the cells doing a transient homing to the lung. Through confocal microscopy, markings compatible with the qtracker on the spinal cord of this animal were visualized.

The literature varies in relation to the time it takes the cell to reach its target organ, MOTHE and collaborators in 2011 [3] screened neural progenitor cells derived from spinal cord and MSCs derived from bone marrow after intrathecal transplantation by lumbar puncture in a spinal cord injury model and found a greater number of cells transplanted into the spinal cord at 27 days compared to 13 and 17 days. In our study the cells were tracked at 7 days post transplantation.

Further studies should be done to explore the potential for cell migration at other time frames, such as 24 hours, 30 days after transplantation. It would also be interesting to evaluate cell migration without the production of tissue injury as compared to the results found in the present study.

In rats, the sequestration of MSCs in pulmonary capillaries has been demonstrated, probably due to the large size of the cells in relation to the capillaries [19] and their low deformation capacity [17].

In the study by GAO et al., 2001 [17], immediately after the intrarterial, intravenous or intraperitoneal transplant of MSCs marked with 111In-oxine, only lung marking was observed. After 48 hours, intense liver staining and less lung staining were observed compared to the analysis immediately after transplantation. Kidneys and spleen also showed radioactivity within 48 hours.

In our study, we did not observe spleen marking, but we did have positive results regarding kidneys and livers.

The fact that cell transplantation occurred shortly after the surgical procedure and therefore, of tissue injury, makes the microenvironment hostile for transplanted cells [22]. It is important to note that, due to the methods used in the present study, it is not possible to determine whether the marked cell is alive or dead, mainly because it is a xenotransplant.

However, the immunohistochemical evaluation (IHQ) for the presence of the macrophage marker was negative for kidneys, lung, brain, spleen and liver, which can attest that the perceived fluorescence comes from the cell that has migrated systemically. The IHQ technique had a low positive for the presence of macrophages in spinal cords, which may suggest that MSC migrated to the injury site and did not provoke a local cellular immune response.

In the case of cell death and consequent phagocytosis by the mononucleated cell, the Qtracker in the cytoplasm of the MSC can mark the defense cells and the perceived fluorescence is due to the migration of the mononuclear cell.

Surprisingly, a large number of animals were marked in the brain. Six brains out of seven were positive for the presence of fluorescence and the presence of labeled cells was confirmed by the confocal microscopy of two brains. These findings may corroborate the migration of MSCs to the brain and justify the use of this route in cell transplants in the clinical cases of brain disorders.

CONCLUSION

AdMSCs are able to migrate from the epidural space and reach target organs such as the injured spinal cord and brain, so that the epidural route is an alternative for cell transplantation to systemic routes such as the intravenous or intrarterial route in the context of inflammatory diseases of the nervous system. It is a viable and safe alternative because it does not require an invasive

surgical procedure to perform cell transplantation, sedation is sufficient to perform the technique. Further studies need to be conducted in order to assess the potential for functional recovery, neuro-regenerative role and safety of the technique before the procedure is used in the clinical routine.

CONFLICT OF INTERESTS

The authors deny conflict of interest

FINANCING

This study was financed in part by the Coordenação de Aperfeiçoamento de Pessoal de Nível Superior - Brasil (CAPES) - Finance Code 001.

REFERENCES

1. Barbash, i.m.; chouraqui, p.; baron, j.; feinberg, m.s.; etzion, s.; tessone, a.; miller, l.; guetta, e.; zipori, d.; kedes, l.h.; et al. Systemic delivery of bone marrow-derived mesenchymal stem cells to the infarcted myocardium: feasibility, cell migration, and body distribution. *Circulation*, v. 108, p. 863–868, 2003.

2. Constantin, g.; marconi s.; rossi, b.; angiari, s.; calderan, l.; anghileri, e.; gini, b.; bach, s. d.; lo, m. m.; bifari, f.; galie, m.; turano. e.; budui, s.; sbarbati, a.; KRAMPERA, M.; BONETTI, B. Adipose-Derived Mesenchymal Stem Cells Ameliorate Chronic Experimental Autoimmune Encephalomyelitis, *stem cell translational and clinical research,*; v.27, p. 2624–2635, 2009.

3. Mothe AJ, Bozkurt G, Catapano J, Zabojova J, Wang X, Keating A, Tator CH, Intrathecal transplantation of stem cells by lumbar puncture for thoracic spinal cord injury in the rat. Spinal Cord. 2011. 49: 967–73.

4. Gattegno-ho, d.; argyle, s. a.; argyle, d. j. Stem cells and veterinary medicine: Tools to understand diseases and enable tissue regeneration and drug discovery. *The Veterinary Journal,* v. 191, p. 19-27, 2012.

5. Hoffman AM, Dow SW. Concise Review: Stem Cell Trials Using Companion Animal Disease Models. *Stem Cells*. 2016;34(7):1709-1729. doi:10.1002/stem.2377

6. Bach FS, Rebelatto CLK, Fracaro L, Senegaglia AC, Fragoso FYI, Daga DR, Brofman PRS, Pimpão CT, Engracia Filho JR, Montiani-Ferreira F, Villanova JA Jr. Comparison of the Efficacy of Surgical Decompression Alone and Combined With Canine Adipose Tissue-Derived Stem Cell Transplantation in Dogs With Acute Thoracolumbar Disk Disease and Spinal Cord Injury. Front Vet Sci. 2019 Nov 8;6:383.

7. Khan S, Rawat T, Kumar R, Chandra V, Saxena, a c, Pawde AM, Kinjavdekar P, Amarpal A, Sharma, GT. Clinical evaluation following the percutaneous transplantation of allogenic bone marrow-derived mesenchymal stem cells (aBM-MSC) in dogs affected by vertebral compression fracture*. Veterinary and Animal Science*. (2020); 10. 100152. 10.1016/j.vas.2020.100152.

8. Karp JM, Teo GSL, Mesenchymal Stem Cell Homing:The Devil Is in the Details. *cell stem cell.* 2009; 4: 206-16.

9. Diacovo, t.; roth, s.; buccola, j.; bainton, d.; springer, t. Neutrophil Rolling, Arrest, and Transmigration Across Activated, Surface Adherent Platelets Via Sequential Action of P-Selectin and the &Integrin CDllb/CDl8. *Blood*. v. 88, p.146-157, 1996.

10. De becker A, Van hummelen P, Bakkus, M, Vande broek, I, De wever, J, De waele, M, Van riet, I. Migration of culture-expanded human mesenchymal stem cells through bone marrow endothelium is regulated by matrix metalloproteinase-2 and tissue inhibitor of metalloproteinase-3. Haematologica. 2007.92; 440–49.

11. Potapova IA, Brink PR, Cohen IS, Doronin SV. Culturing of human mesenchymal stem cells as three-dimensional aggregates induces functional expression of CXCR4 that regulates adhesion to endothelial cells. *J Biol Chem*. 2008;283(19):13100-13107. doi:10.1074/jbc.M800184200

12. Sohni A, Verfaillie C M. Mesenchymal Stem Cells Migration Homing and Tracking. Stem Cells International, 2013;. 8.

13. Rüster B, Göttig S, Ludwig RJ, et al. Mesenchymal stem cells display coordinated rolling and adhesion behavior on endothelial cells. Blood. 2006;108(12):3938-44. doi:10.1182/blood-2006-05-025098

14. Fox, JM, Chamberlain, G, Ashton, BA, Middleton, J. Recent advances into the understanding of mesenchymal stem cell trafficking. Br J Haemat. 2007;137(4):491–502.

15. Zhang D, Fan GC, Zhou X, et al. Over-expression of CXCR4 on mesenchymal stem cells augments myoangiogenesis in the infarcted myocardium. *J Mol Cell Cardiol*. 2008;44(2):281-292.

16. Leibacher J, Henschler R. Biodistribution, migration and homing of systemically applied mesenchymal stem/stromal cells StemCell Research&Therapy 2016.7: 7.

17. Gao J, Dennis JE, Muzic RF, Lundberg M, Caplan AI. The dynamic in vivo distribution of bone marrow-derived mesenchymal stem cells after infusion. *Cells Tissues Organs*. 2001;169(1):12-20. doi:10.1159/000047856
18. Kraitchman DL, Tatsumi M, Gilson WD, et al. Dynamic imaging of allogeneic mesenchymal stem cells trafficking to myocardial infarction. *Circulation*. 2005;112(10):1451-1461. doi:10.1161/CIRCULATIONAHA.105.537480

19. Schrepfer S, Deuse T, Reichenspurner H, Fischbein M P, Robbins, R C, Pelletier, MP. Stem cell transplantation: the Lung barrier. Transplantation Proceedings.2007. 39; 573–76.

20. Satake K, Lou J, Lenke LG. Migration of mesenchymal stem cells through cerebrospinal fluid into injured spinal cord tissue. Spine . 2004;29(18):1971-1979. doi:10.1097/01.brs.0000138273.02820.0a

21. Deng Y B, Liu, XG, Liu, ZG, Liu, XL, Liu, Y, Zhou, GQ. Implantation of BM mesenchymal stem cells into injured spinal cord elicits de novo neurogenesis and functional recovery: evidence from a study in rhesus monkeys. *Cytotherapy,* 2006. 8; 210-14.

22. bakshi, a.; barshinger, a. l.; swanger, s. a.; madhvani, v.; shumsky, j. s.; neuhuber, b.; fischer, I. Lumbar Puncture Delivery of Bone Marrow Stromal Cells in Spinal Cord Contusion: A Novel Method for Minimally Invasive Cell Transplantation. *Journal of Neurotrauma,* v. 23, n.1, p. 55–65, 2006. doi:10.1089/neu.2006.23.55

23. paul, c.; samdani, a.f.; betz, r.r.; fischer, i.; neuhuber, b. Grafting of human bonemarrow stromal cells into spinal cord injury: a comparison of delivery methods. *Spine* v.4 p. 328-334,2009.

24. Triffterer L, Marhofer P, Lechner G, Marksz TC, Kimberger O, Schmid W, Marhofer D. An observational study of the macro- and micro-haemodynamic implications of epidural anaesthesia in children. Anaesthesia. 2017 Apr;72(4):488-495.

25. Burm, AGL. "Clinical pharmacokinetics of epidural and spinal anaesthesia." Clinical pharmacokinetics 16.5 (1989): 283-311.

26. Pleuvry, Barbara J. "Factors affecting drug absorption and distribution." *Anaesthesia & Intensive Care Medicine* 6.4 (2005): 135-138.

27. Franzoni MS, Brandi A, de Oliveira Matos Prado JK, Elias F, Dalmolin F, de Faria Lainetti P, Prado MCM, Leis-Filho AF, Fonseca-Alves CE. Tumor-infiltrating CD4+ and CD8+ lymphocytes and macrophages are associated with prognostic factors in triple-negative canine mammary complex type carcinoma.

Res Vet Sci. 2019 Oct;126:29-36. doi: 10.1016/j.rvsc.2019.08.021. Epub 2019 Aug 13. PMID: 31425936.

28. Vanický, I. et al. A simple and reproducible model of spinal cord injury induced by epidural balloon infl ation in the rat. Journal of Neurotrauma, 2001, 8,(12);1399-1407.

29. Muller-Borer, BJ, collins MC, Gunst, PR, et al. Quantum dot labeling of mesenchymal stem cells. J. Nanobiotechnol. 2007;9.

30. Carvalho AM, Yamada ALM, Golim M A, Álvarez LEC, Hussni CA, Alves AL G. Evaluation of mesenchymal stem cell migration after equine tendonitis therapy. Equine veterinary journal 2013; 46: 635-38.

31. Walczak P, Zhang J, Gilad AA, et al. Dual-modality monitoring of targeted intraarterial delivery of mesenchymal stem cells after transient ischemia. *Stroke*. 2008;39(5):1569-1574. doi:10.1161/STROKEAHA.107.502047